JOURNAL OF SOLID STATE CHEMISTRY **112**, 355–361 (1994)

Neutron Powder Diffraction Study of the Crystal Structures of Sr_2RuO_4 and Sr_2IrO_4 at Room Temperature and at 10 K

Q. Huang,*,† J. L. Soubeyroux,* O. Chmaissem,* I. Natali Sora,* A. Santoro,* R. J. Cava,‡
J. J. Krajewski,‡ and W. F. Peck, Jr.‡

**National Institute of Standards and Technology, Gaithersburg, Maryland 20899; †University of Maryland, College Park, Maryland 20742; and ‡AT&T Bell Laboratories, Murray Hill, New Jersey 07974*

Received November 1, 1993; accepted January 20, 1994

The crystal structures of the compounds Sr_2RuO_4 and Sr_2IrO_4 have been analyzed at room temperature and at 10 K with the neutron powder diffraction technique and the Rietveld method of profile fitting. Sr_2RuO_4 crystallizes with the symmetry of space group *I4/mmm* and room temperature lattice parameters a = 3.8730(3) and c = 12.7323(9) Å, while Sr_2IrO_4 has the symmetry of space group $I4_1/acd$ and lattice parameters a = 5.4994(1) and c = 25.7841(8) Å. The unit cells of the two compounds are related to one another by the transformation matrix (1, −1, 0/1, 1, 0/0, 0, 2). The main difference between the two structures is that the MO_6 octahedra (M = Ru, Ir) have a regular, undistorted configuration in the ruthenium compound, while they are tilted by about 11° around the c axis of the unit cell in the iridium compound. The oxygen atoms of the IrO_2 layers were found to be disordered over two sets of positions $x, x, \frac{1}{4}$ with $x = \frac{1}{4} \pm \delta$. This means that the IrO_6 octahedra assume two configurations and on a local level their relative orientation does not obey the symmetry requirements of space group $I4_1/acd$ in all cases. The MO_6 octahedra are elongated along the c axis, and this distortion is more pronounced in Sr_2RuO_4 than in Sr_2IrO_4. The coordination of the strontium atoms is ninefold in both compounds. Because of the tilting of the IrO_6 octahedra, however, the coordination polyhedra are different in the two cases. No phase transitions have been observed down to 10 K in either compound. © 1994 Academic Press, Inc.

INTRODUCTION

Transition metal oxides with the layered K_2NiF_4 structure type have long been studied because they display a variety of unusual structural and magnetic properties (1). More recently, they have been of interest also as analogs to the superconducting materials derived from La_2CuO_4. Although the members with the first row of transition metals are commonly known, the detailed properties of the 4*d*- and 5*d*-based compounds of the same family remain largely unexplored. Of these, Sr_2RuO_4 and Sr_2IrO_4 (2, 3) stand out because the former has surprisingly good metallic conductivity (4), while the latter has insulating behavior unexpected for Ir^{4+} (with five d electrons) in an ideal tetragonal K_2NiF_4-type structure.

In previous reports (2, 3), the symmetry of space group *I4/mmm* was assigned to both compounds. However, studies of the metal–insulator transition in the $Sr_2Ru_{1-x}Ir_xO_4$ solid solution suggested that Sr_2RuO_4 and Sr_2IrO_4 are not isostructural (5). This result was corroborated in a more recent study of Sr_2IrO_4 in which it was found that this compound crystallizes with the symmetry of space group $I4_1/acd$ (6). In order to further clarify this point, and to find a possible structural explanation for the puzzling insulating character of Sr_2IrO_4, we carried out a determination of the crystal structures of both the ruthenium and iridium compounds by powder neutron diffraction, at 300 and 10 K. The results of this analysis, reported in the following sections, showed that Sr_2RuO_4 does indeed crystallize with the ideal tetragonal K_2NiF_4 structure, while Sr_2IrO_4 has a larger unit cell of different symmetry, due to the rotation of the corner-sharing octahedra about an axis parallel to c. This may result in a decreased metal–oxygen–metal orbital overlap and thus explain the insulating properties of Sr_2IrO_4.

EXPERIMENTAL

The compounds Sr_2RuO_4 and Sr_2IrO_4 were synthesized from $SrCO_3$, IrO_2, and RuO_2 mixed in stoichiometric proportions. The mixtures were heated in flowing O_2 at 900°C for 24 hr, 1000°C for 24 hr and 1100°C for 60 hr, with intermediate grindings. In the case of Sr_2RuO_4 an additional treatment at 1200°C for 24 hr was employed.

Neutron powder diffraction data were collected at room temperature and at 10 K with the 32-counter high-resolution powder diffractometer at the reactor of the National Institute of Standards and Technology, using the experimental conditions listed in Table 1. The observed intensities from the iridium compound were corrected for absorption using the correction factors for cylinders (7) and

0022-4596/94 $6.00

TABLE 1
Collection of Intensity Data

Monochromatic beam	311 reflection of a Cu monochromator
Wavelength	1.540(1) Å
Horizontal divergences	15′, 20′, 7′ of arc for the in-pile, monochromatic beam, and diffracted beam collimators, respectively
Sample container	Vanadium or aluminium cans of about 10 mm diameter
2θ angular range	5°–165°, steps: 0.05°
Scattering amplitudes (10^{-12} cm)	b(Sr) = 0.702, b(Ru) = 0.721, b(Ir) = 1.060, b(O) = 0.581

Note. Data were collected at room temperature and at 10 K.

the value of $\mu R = 0.4$ was determined experimentally (due to the small absorption cross section of Ru, no absorption correction was made for Sr_2RuO_4). The reflections of Sr_2RuO_4 could be indexed on a tetragonal cell with lattice parameters $a_p \times a_p \times 3a_p$ Å^3, where a_p is the parameter of cubic perovskite (about 4 Å), while the presence of weak extra reflections in the powder pattern of Sr_2IrO_4 were consistent with a unit cell of parameters $a_p\sqrt{2} \times a_p\sqrt{2} \times 6a_p$. This is a strong indication that the first compound has the K_2NiF_4-type structure and the symmetry of space group *I*4/*mmm* (8), while the second may have the symmetry of space group *I*4$_1$/*acd* (6) and be isostructural with Ca_2MnO_4 (9, 10). Refinements of the two structures were based on these assumptions and were made using the program GSAS of Larson and Von Dreele [11].

The initial parameters of Sr_2RuO_4 were derived from the basic atomic arrangement of the K_2NiF_4-type structure, assuming the symmetry of space group *I*4/*mmm*, as we have mentioned earlier. Refinements of this model gave good agreement between observed and calculated intensities. The data collected at 10 K showed that the compound does not have any phase transitions down to this temperature. The thermal factors of all atoms did not present any unusual behavior, indicating that there is no significant disorder in the structure. The structural parameters at room temperature and at 10 K are given in Table 2, and Fig. 1 shows the plot of the observed and calculated intensities for the room temperature experiment.

As mentioned previously, the initial model of the structure of Sr_2IrO_4 was assumed to be similar to that of Ca_2MnO_4 (9, 10) and refinements were carried out adopting the symmetry of space group *I*4$_1$/*acd*. The results of these calculations gave acceptable values of the agreement factors *R*. The temperature factor of the oxygen atoms of the IrO_2 layer, however, was significantly larger than that of the oxygen atoms on the SrO plane (1.05 vs 0.36 and 0.76 vs 0.09 Å^2, for the room temperature and the 10 K experiments, respectively). In addition, the agreement between observed and calculated intensities for some reflections was poorer than one would expect in a well-refined structure, indicating that not all the initial structural details were modeled properly. A possible explanation of these results may be found in a disordering of the atomic arrangement of the IrO_2 layers. More specifically, the shift of the oxygen atoms from the positions $\frac{1}{4}$, $\frac{1}{4}$, $\frac{1}{4}$, which they would occupy if the symmetry were *I*4/*mmm*, causes a rotation of the IrO_6 octahedra about a direction parallel to the *c* axis of the unit cell. The rotation

TABLE 2
Structural Parameters and Refinement Indices for Sr_2RuO_4 at Room Temperature (First Line) and at 10 K (Second Line)

Space group: *I*4/*mmm*, a = 3.8730(3) Å, c = 12.7323(9) Å, V = 190.98(4) Å^3;
3.86358(7) Å, 12.7155(4) Å, 189.807(9) Å^3.

Atom	Position	x	y	z	B (Å^2)	Occupancy
Sr	4e 4*mm*	0	0	0.3525(2)	0.59(4)	1
		0	0	0.3526(2)	0.14(4)	1
Ru	2a 4/*mmm*	0	0	0	0.72(5)	1
		0	0	0	0.50(5)	1
O(1)	4c *mmm*	0	$\frac{1}{2}$	0	0.66(5)	1
		0	$\frac{1}{2}$	0	0.32(4)	1
O(1)	4e 4*mm*	0	0	0.1624(2)	0.96(5)	1
		0	0	0.1625(2)	0.60(5)	1

Note. R_p(%) = 9.00 R_{wp}(%) = 12.09 χ = 1.22
8.92 12.15 1.22

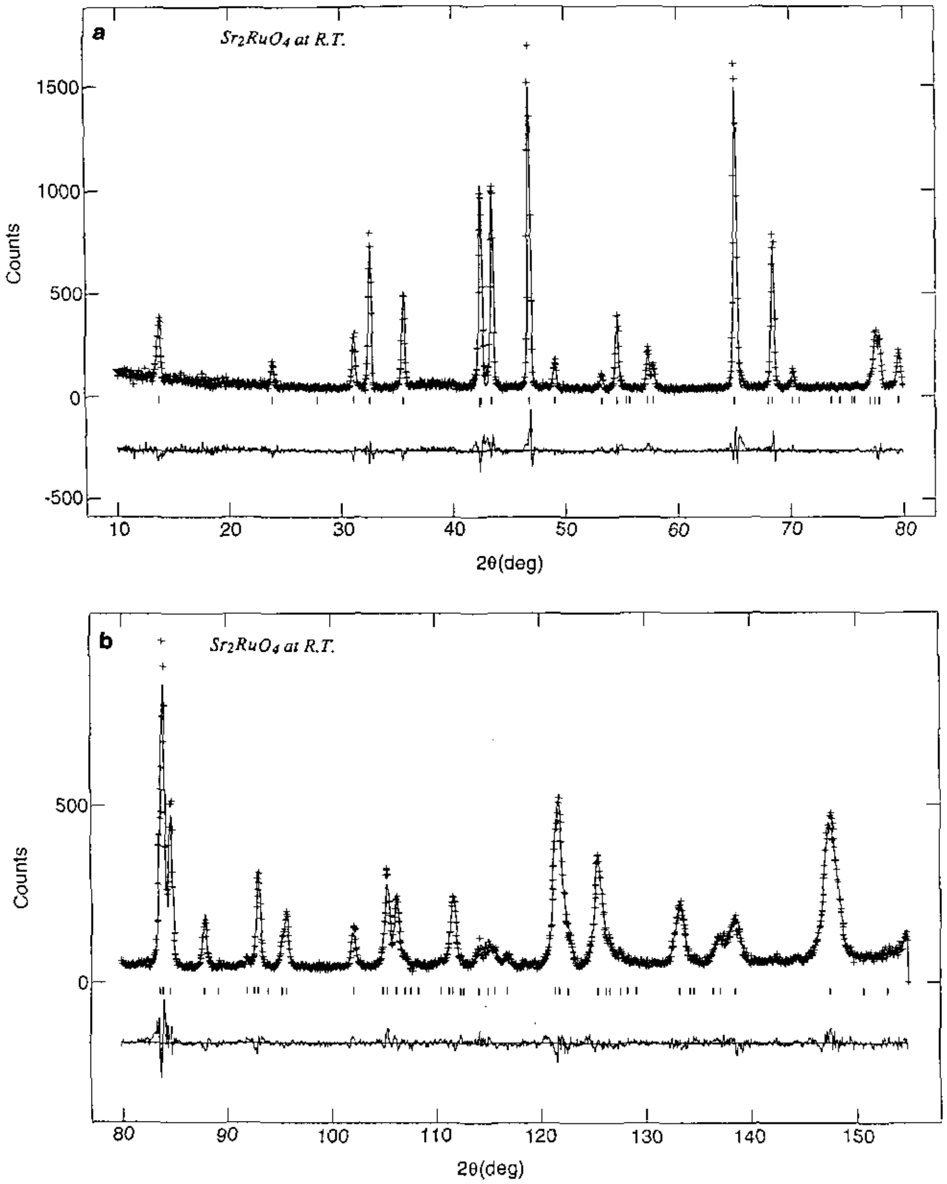

FIG. 1. Plot of the observed (+) and calculated (continuous line) intensities obtained at room temperature from the sample of Sr_2RuO_4. The difference plot is shown at the bottom of the figure. For clarity, the low-angle and high-angle plots have different scales in the y axis (neutron counts). The same is true for Fig. 3.

may be clockwise or counterclockwise, and choosing one sense or the other results in the same structure with a shift of the origin of $\frac{1}{2}$ along c. In the ordered structure, the arrangement of the oxygen atoms obeys the symmetry requirements of the screw axis 4_1 parallel to c. However, since successive IrO_2 layers are separated along c by a distance of about 6.5 Å, we may assume that they are uncorrelated and that the IrO_6 octahedra may be rotated one with respect to the other in either the clockwise or the counterclockwise configuration, independent of symmetry. As shown in Fig. 2, this is equivalent to disordering the oxygen atoms of the IrO_2 planes over two sets of positions x, x, $\frac{1}{4}$, with $x = 0.25 \pm \delta$, where δ determines the angle of rotation of the octahedra with respect to the orientation they would have if the symmetric positions $\frac{1}{4}$, $\frac{1}{4}$, $\frac{1}{4}$ were occupied. In the average structure, as seen in a diffraction experiment, the two sets of positions will appear to be partially occupied, although, on a local level, only one set of sites can be filled in each layer, because of constraints imposed by the oxygen–oxygen separations. Refinements of a model with the IrO_2 oxygen atoms disordered as described above gave agreement factors R

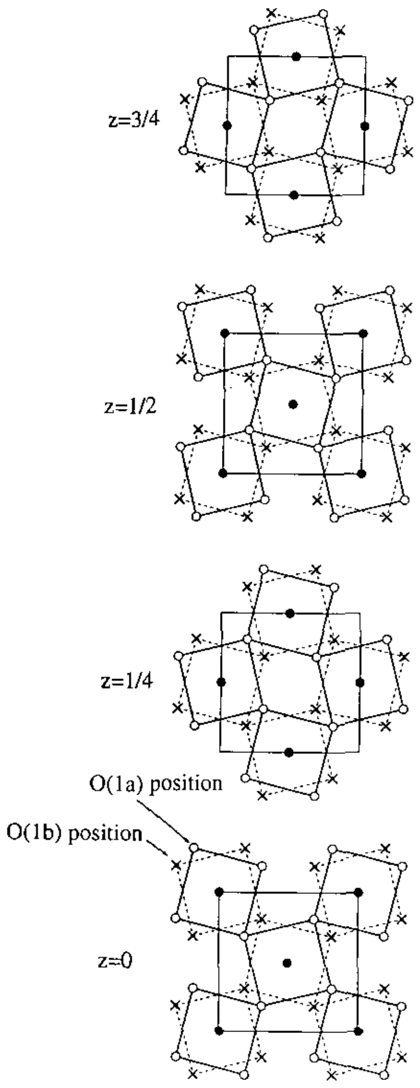

FIG. 2. Successive IrO_2 layers along *c* in the structure of Sr_2IrO_4. The full circles represent the iridium atoms, located at the center of IrO_6 octahedra. The circles and the crosses represent the two sets of positions over which the oxygen atoms are distributed. The oxygen atoms of the SrO layers directly above and below each iridium atom are not represented for clarity.

(R_p = 7.88 and R_w = 9.67) significantly better than those corresponding to the ordered structure (R_p = 8.54 and R_w = 10.22) and quite reasonable values of the temperature factors. The results of these calculations are listed in Table 3, and the plot of observed and calculated intensities is shown in Fig. 3 for the room temperature run. In Table 4 the relevant bond distances are given for both the Ru and the Ir compounds.

RESULTS AND DISCUSSION

(*a*) Sr_2RuO_4

The structure of Sr_2RuO_4 is schematically shown in Fig. 4. It may also be represented by the sequence of layers,

$$\cdots[(RuO_2)_o(SrO)_c(SrO)_o(RuO_2)_c(SrO)_o(SrO)_c](RuO_2)_o\cdots,$$

where the symbols in each parenthesis give the chemical composition of the layer, the subscripts o and c indicate if the cation is at the origin or in the center of the layer's mesh, and the square brackets include the content of one unit cell (12). This atomic arrangement is practically identical to that of La_2CuO_4 (13). Ruthenium is sixfold coordinated and the coordination polyhedron may be described as an elongated octahedron with distances Ru–O(1) = 1.9364(1) Å and Ru–O(2) = 2.067(3) Å. This arrangement is significantly more regular than that found, for example, in La_2CuO_4 (13) and $La_{1.85}Sr_{0.15}CuO_4$ (14), where these two distances range from 1.896 to 2.398 Å and from 1.890 to 2.412 Å, respectively. Strontium is nine-coordinated and the coordination polyhedron is a capped square antiprism with the Sr atom displaced considerably from the antiprism center toward the capped face, a feature also present in La_2CuO_4 and in its Sr- and Ba-doped derivatives. As shown in Table 2, no phase transition was detected for this compound down to 10 K.

(*b*) Sr_2IrO_4

The structure of Sr_2IrO_4 is basically similar to that of the ruthenium compound and is illustrated in Fig. 5. The tilting of the IrO_6 octahedra around the *c* axis causes a change of the unit cell with lattice parameters related to those of the ruthenium compound by the transformation matrix (1, −1, 0/1, 1, 0/0, 0, 2). As we have mentioned earlier, the oxygen atoms located on the IrO_2 planes are disordered over two sets of positions $x, x, \frac{1}{4}$, with $x = \frac{1}{4} \pm \delta$. On any given layer, only the sites of one set can be occupied because any other distribution would result in unreasonably short oxygen–oxygen distances. The values of δ found at room temperature and at 10 K (0.0502 and 0.0519) correspond to a tilt angle α of 11.36° and 11.72°, respectively, as indicated in Fig. 6. Since the octahedra in each layer share corners, they are all rotated one with respect to the other consistently with the constraints imposed by this structural feature. The sites occupied by oxygen in the next layer IrO_2 along *c* can be either those generated from the previous ones by the operation of the 4_1 axis (83% of the cases) or those belonging to the second set and uncorrelated to the former ones by any symmetry operation of the space group (17% of the cases). On the basis of this model it is therefore possible to view the structure as built of short-range domains in which the IrO_6 octahedra have one of the two possible configurations (e.g., the one with the octahedra of the zero level tilted clockwise) mixed with domains in which they have the other configuration. The fact that the occupancies of the oxygen atoms O(1) on the IrO_2 layers are not equal is an indication that the extent of the disorder in the structure is a function of the preparation conditions. This conclu-

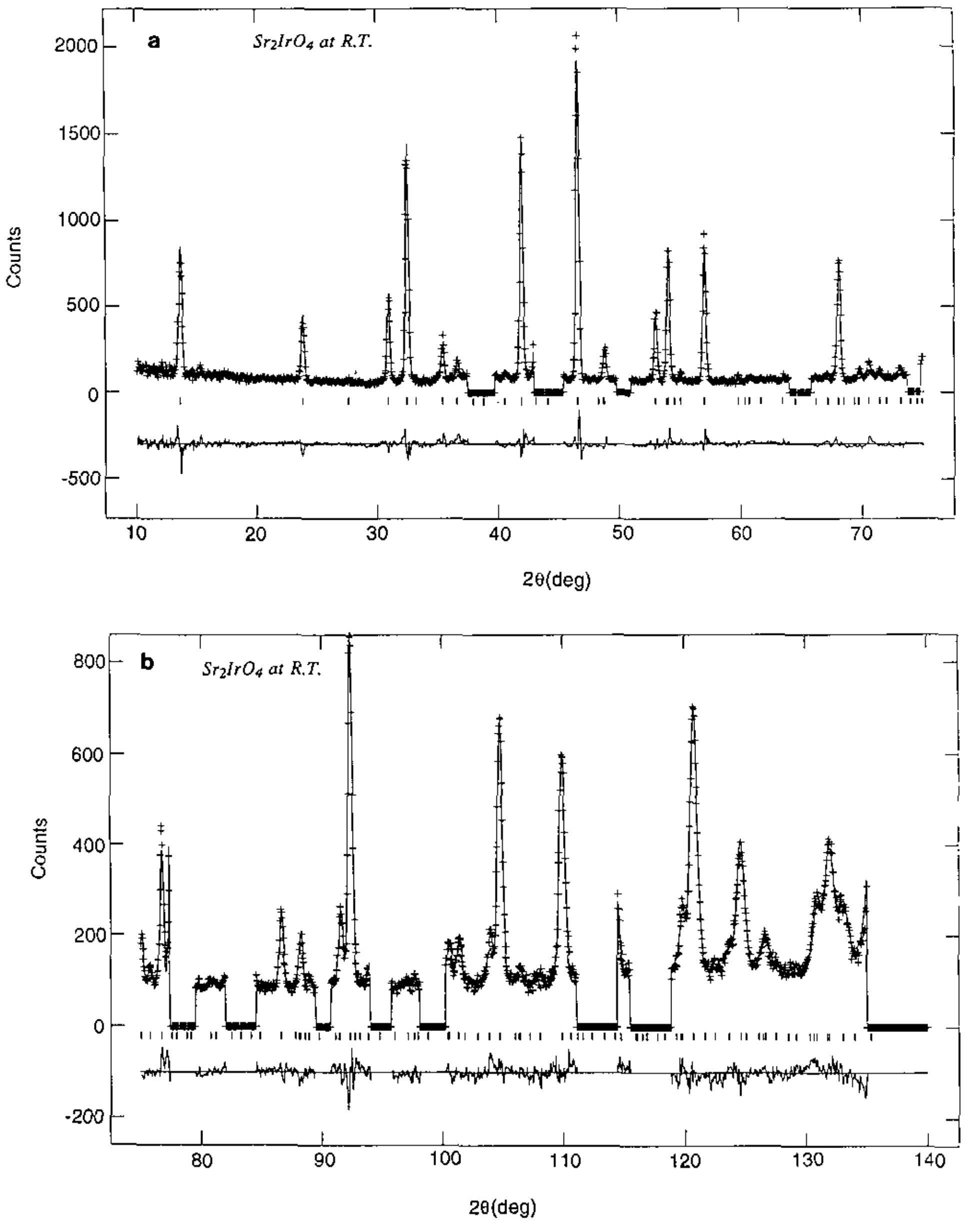

FIG. 3. Plot of observed (+) and calculated (continuous line) intensities obtained at room temperature from the sample of Sr_2IrO_4. The excluded regions are those affected by extra intensities due to impurities in the sample. The difference plot is shown at the bottom of the figure.

sion may explain why a similar disordering of the oxygen atoms has not been reported in other compounds (such as Ca_2MnO_4 (9, 10)) isostructural with Sr_2IrO_4.

The IrO_6 octahedra are significantly less elongated than those of ruthenium. More specifically, the distances Ir–O(1) = 1.983 Å and Ir–O(2) = 2.067 Å give a difference Δ = 0.084 Å, compared with a value of 0.131 Å in Sr_2RuO_4. The tilting of the IrO_6 octahedra results in a different coordination of the strontium atoms in the two compounds. As shown in Table 4, there are four separations Sr–O of 2.698 Å in Sr_2RuO_4, while in the iridium compound these separate into two short (2.473 Å) and two long (3.026 Å) distances, due to the rotation of the octahedra around the *c* axis. However, the valence of strontium, calculated with the formalism and the constants of Brown and Altermatt (15, 16), remains practically the same, being 2.01 v.u. for Sr_2RuO_4 and 2.06 v.u. for Sr_2IrO_4.

The crystal structures of Sr_2RuO_4 and Sr_2IrO_4 provide a framework for the interpretation of the physical properties of these materials. First of all, the two compounds are not isostructural, thus explaining the unusual composition dependence of the lattice parameters in the $Sr_2Ru_{1-x}Ir_xO_4$ solid solution (5). For Sr_2RuO_4 the Ru–O–Ru in-plane

TABLE 3
Structural Parameters and Refinement Indices for Sr_2IrO_4 at Room Temperature (First Line) and at 10 K (Second Line)

Space group: $I4_1/acd$, a = 5.4994(1) Å, c = 25.7841(8) Å, V = 779.81(4) Å^3;
5.48463(9) Å, 25.7977(7) Å, 776.03(4) Å^3.

Atom	Position	x	y	z	B (Å^2)	Occupancy
Sr	16d 2 . .	0	0	0.17537(8)	0.91(4)	1
		0	0	0.17573(6)	0.26(3)	1
Ir	8a $\bar{4}$ . .	0	0	0	0.70(4)	1
		0	0	0	0.41(4)	1
O(1a)	16f . . 2	0.1998(4)	0.1998(4)	$\frac{1}{4}$	0.68(6)[a]	0.833(8)
		0.1981(3)	0.1981(3)	$\frac{1}{4}$	0.32(5)	0.861(7)
O(1b)	16f . . 2	0.3002(4)	0.3002(4)	$\frac{1}{4}$	0.68(6)	0.167(8)
		0.3019(3)	0.3019(3)	$\frac{1}{4}$	0.32(5)	0.139(7)
O(2)	16d 2 . .	0	0	0.0802(1)	0.92(5)	1
		0	0	0.07974(7)	0.34(4)	1

$R_p(\%)$ = 7.88 $R_{wp}(\%)$ = 9.67 χ = 1.29
7.88 9.60 1.23

[a] Constrained such that $B(O(1a)) = B(O(1b))$ and $n(O(1a)) = 1 - n(O(1b))$.

bonding has an angle of 180°. Although the electronic band structure has not yet been calculated, we expect that the conductivity arises from a broad, partially occupied electronic band of primarily Ru 4d character, with some oxygen 2p admixture.

The crystal structure of Sr_2IrO_4 suggests two possible explanations for its electrically insulating nature. First the elongation of the Ir–O(2) bonds along the c axis probably splits the t_{2g} orbitals into a degenerate xz and yz pair, and an xy orbital at higher energy. If the bands are narrow enough and the splitting large enough, the five 5d electrons

TABLE 4
Selected Interatomic Distances (Å) in Sr_2RuO_4 and Sr_2IrO_4

	Room temperature		10 K	
		Sr_2RuO_4		
Sr–O(1)	×4	2.698(1)	×4	2.692(1)
Sr–O(2)		2.420(3)		2.418(3)
Sr–O(2)	×4	2.745(3)	×4	2.739(2)
Ru–O(1)	×4	1.9364(1)	×4	1.93179(4)
Ru–O(2)	×2	2.067(3)	×2	2.066(3)
		Sr_2IrO_4		
Sr–O(1a)	×1.67(2)	2.473(3)	×1.72(1)	2.456(2)
Sr–O(1a)	×1.67(2)	3.026(2)	×1.72(1)	3.026(2)
Sr–O(1b)	×0.33(2)	2.473(3)	×0.28(1)	2.456(2)
Sr–O(1b)	×0.33(2)	3.026(2)	×0.28(1)	3.026(2)
Sr–O(2)		2.455(3)		2.476(2)
Sr–O(2)	×4	2.7534(2)	×4	2.7459(1)
Ir–O(1a)	×3.33(3)	1.9832(6)	×3.44(3)	1.9804(5)
Ir–O(1b)	×0.67(3)	1.9832(6)	×0.56(3)	1.9804(5)
Ir–O(2)	×2	2.067(3)	×2	2.057(2)

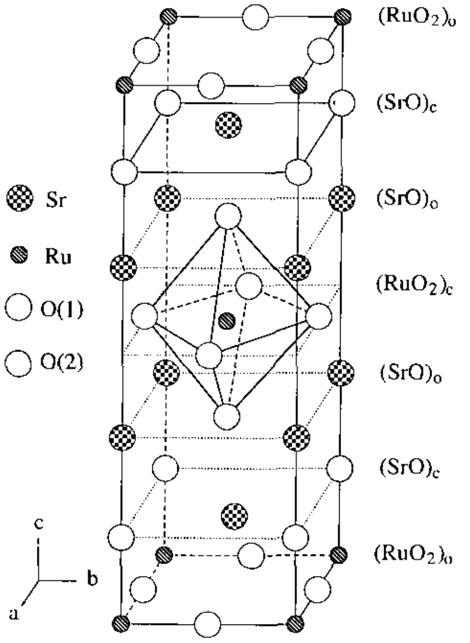

FIG. 4. Schematic representation of the unit cell of Sr_2RuO_4.

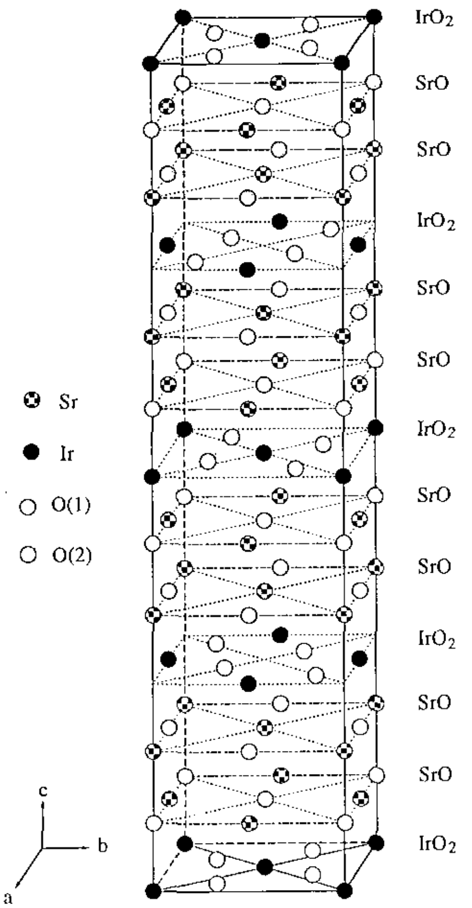

FIG. 5. Schematic representation of the unit cell of Sr_2IrO_4. The unit cell of this compound is related to that of Sr_2RuO_4 by the transformation matrix (1, − 1, 0/1, 1, 0/0, 0, 2). Consistently with the data of Table 3, the origin of the unit cell is taken at $\bar{4}c2_1$.

would result in half filling the *xy* orbital, suggesting that the insulating character comes from electron–electron correlation in a half-filled band. An alternate explanation can be found in the rotations of the IrO_6 octahedra, which cause a significant deviation of the Ir–O(1)–Ir bond angle from 180° (to approximately 157°), significantly decreasing the electronic bandwidth due to decreased metal–oxygen–metal orbital overlap. This has been seen to result in insulating behavior in other systems, e.g., $LnNiO_3$ [17]. This band narrowing could further enhance the possibility for half filling of the *xy* orbitals.

The average Ir–O bond length (2.01 Å) is only 1.4% longer than that of Ru–O (1.98 Å): if the driving force causing a twisted IrO_2 plane in Sr_2IrO_4 and an orthogonal RuO_2 plane in Sr_2RuO_4 is geometrical, having to do with a difference in size between SrO and MO_2 layers, then the iridium and ruthenium compounds should be considered as bordering on structural instability and each structure should be barely stable with respect to the other.

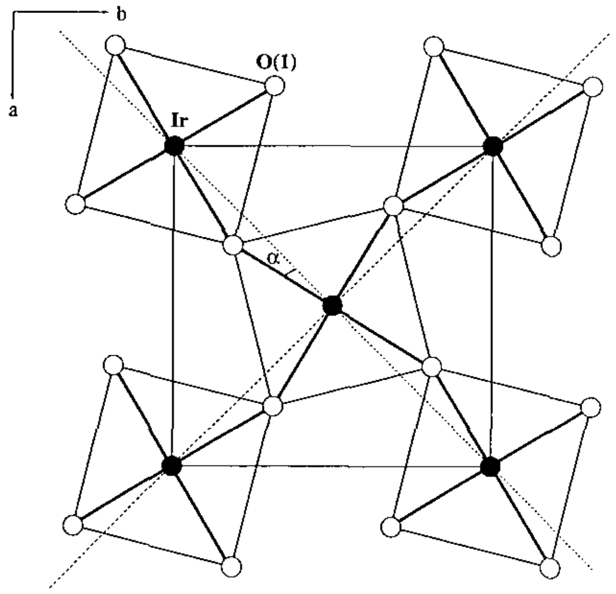

α = 11.36(8)° at R.T.
α = 11.72(7)° at 10K

FIG. 6. IrO_2 layer in the structure of Sr_2IrO_4 showing the mutual orientation of the IrO_6 octahedra and the values of the angle α of rotation of the octahedra around the *c* axis.

REFERENCES

1. J. B. Goodenough and J. M. Longo, *in* "Landolt–Bornstein: Numerical Data and Functional Relationships in Science and Technology, New Series," Group III (K. H. Hellwege, Ed.), Vol. 4a, p. 126. Springer–Verlag, Berlin, 1970.
2. J. J. Randall, Jr., L. Katz, and R. Ward, *J. Am. Chem. Soc.* **79,** 266 (1957).
3. J. J. Randall and R. Ward, *J. Am. Chem. Soc.* **81,** 2629 (1959).
4. F. Lichtenberg, A. Catana, J. Mannhart, and D. G. Schlom, *Appl. Phys. Lett.* **60,** 1138 (1992).
5. R. J. Cava, B. Batlogg, K. Kiyono, H. Takagi, J. J. Krajewski, W. F. Peck, Jr., L. W. Rupp, Jr., and C. H. Chen, *Phys. Rev. B* **49,** 11890 (1994).
6. M. Crawford, private communication.
7. "International Tables for X-ray Crystallography," Vol. II. Kynoch Press, Birmingham, 1959.
8. M. Longo and P. M. Raccah, *J. Solid State Chem.* **6,** 526 (1973).
9. M. E. Leonowicz, K. R. Poppelmeier, and J. M. Longo, *J. Solid State Chem.* **59,** 71 (1985).
10. J. Takahashi and N. Kamegashira, *Mater. Res. Bull.* **28,** 565 (1993).
11. A. C. Larson and R. B. VonDreele, "General Structure Analysis System." University of California, 1985.
12. A. Santoro, F. Beech, M. Marezio, and R. J. Cava, *Physica C* **156,** 693 (1988).
13. J. M. Delgado, R. K. McMullan, G. Diaz de Delgado, B. J. Wuensch, P. J. Picone, H. P. Jenssen, and D. R. Gabbe, *Phys. Rev. B* **37,** 9343 (1988).
14. R. J. Cava, A. Santoro, D. W. Johnson, Jr., and W. W. Rhodes, *Phys. Rev. B* **35,** 6716 (1987).
15. I. D. Brown, "Structure and Bonding in Crystals," Vol. II, p. 1. Academic Press, New York, 1981.
16. I. D. Brown, *Phys. Chem. Miner.* **15,** 30 (1987).
17. J. B. Torrance, P. Lacorre, A. I. Nazzal, E. J. Ansaldo, and Ch. Niedermayer, *Phys. Rev. B* **45,** 8209 (1992).